


# Clinical and genetic screening in a large Iranian family with Marfan syndrome: A case study

Farzane Vafaeie<sup>1</sup> | Zahra Miri Karam<sup>2,3</sup> | Abolfazl Yari<sup>1,3</sup> | Hossein Safarpour<sup>1</sup> |  
Tooba Kazemi<sup>4</sup> | Shokoofeh Etesam<sup>5</sup> | Mojtaba Mohammadpour<sup>6</sup> |  
Ebrahim Miri-Moghaddam<sup>4</sup> 

<sup>1</sup>Cellular and Molecular Research Center, Birjand University of Medical Sciences, Birjand, Iran

<sup>2</sup>Physiology Research Center, Institute of Neuropharmacology, Kerman University of Medical Sciences, Kerman, Iran

<sup>3</sup>Department of Medical Genetics, Afzalipour Faculty of Medicine, Kerman University of Medical Sciences, Kerman, Iran

<sup>4</sup>Cardiovascular Disease Research Center, Razi Hospital, Birjand University of Medical Sciences, Birjand, Iran

<sup>5</sup>Department of Biological Sciences, Technical and Vocational University (TVU), Tehran, Iran

<sup>6</sup>Department of Optometry, School of Rehabilitation, Shahid Beheshti University of Medical Sciences, Tehran, Iran

## Correspondence

Ebrahim Miri-Moghaddam, Department of Molecular Medicine, Cardiovascular Disease Research Center, Faculty of Medicine, Razi Hospital, Birjand University of Medical Sciences, Ghaffari Blvd., Birjand, Iran.  
Email: [miri4@bums.ac.ir](mailto:miri4@bums.ac.ir) and [moghaddam4@yahoo.com](mailto:moghaddam4@yahoo.com)

## Abstract

**Background and Aims:** Marfan syndrome (MFS) is an autosomal dominant genetic disorder caused by pathogenic variants of the fibrillin-1-encoding *FBN1* gene that commonly affects the cardiovascular, skeletal, and ocular systems. This study aimed to evaluate the clinical features and genetic causes of the MFS phenotype in a large Iranian family.

**Methods:** Seventeen affected family members were examined clinically by cardiologists and ophthalmologists. The proband, a 48-year-old woman with obvious signs of MFS, her DNA sample subjected to whole-exome sequencing (WES). The candidate variant was validated by bidirectional sequencing of proband and other available family members. In silico analysis and molecular modeling were conducted to determine the pathogenic effects of the candidate variants.

**Results:** The most frequent cardiac complications are mitral valve prolapse and regurgitation. Ophthalmic examination revealed iridodonesis and ectopic lentis. A heterozygous missense variant (c.2179T>C/p.C727R) in exon 19 of *FBN1* gene was identified and found to cosegregate with affected family members. Its pathogenicity has been predicted using several in silico predictive algorithms. Molecular docking analysis indicated that the variant might affect the binding affinity between *FBN1* and *LTBP1* proteins by impairing disulfide bond formation.

**Conclusion:** Our report expands the spectrum of the Marfan phenotype by providing details of its clinical manifestations and disease-associated molecular changes. It also highlights the value of WES in genetic diagnosis and contributes to genetic counseling in families with MFS.

## KEYWORDS

*FBN1*, Marfan syndrome, molecular docking, pathogenic variant, whole exome sequence

Farzane Vafaeie and Zahra Miri Karam contributed equally as the first authors.

This is an open access article under the terms of the Creative Commons Attribution-NonCommercial-NoDerivs License, which permits use and distribution in any medium, provided the original work is properly cited, the use is non-commercial and no modifications or adaptations are made.

© 2023 The Authors. *Health Science Reports* published by Wiley Periodicals LLC.

## 1 | INTRODUCTION

Marfan syndrome (MFS; MIM #154700) is an inherited connective tissue disorder with considerable clinical variability. It is mostly defined by a wide range of clinical signs affecting multiple systems and organs, including the skeletal, ocular, and cardiovascular systems, as well as the skin, lung, and dura. The primary cause of death in patients with MFS is aortic complications.<sup>1</sup> It was first described in 1896 by Antoine-Bernard in a 5-year-old girl with skeletal problems.<sup>2</sup> The incidence rate of MFS is approximately 0.5 to 1 in 5000 individuals in the general population, with no gender or ethnic bias.<sup>3</sup> The clinical diagnosis of MFS is based on a combination of skeletal, ophthalmic, and cardiovascular symptoms and complications along with a positive family history, if available. In the absence of family history, genetic testing may be used to confirm the diagnosis. According to the revised Ghent criteria,<sup>4</sup> several features, including dislocated lenses of the eye and aortic root aneurysm, are sufficient for the unmistakable diagnosis of MFS with or without a positive family history. In most cases, MFS is inherited in an autosomal dominant pattern and is caused by homozygous, heterozygous, and compound heterozygous mutations in the Fibrillin-1 (*FBN1*, OMIM ID: #134797, NCBI Gene ID: 2200) gene. To date, more than 3000 pathogenic variants of *FBN1* have been reported in MFS in the Universal Mutation Database (<http://www.umd.be>). Most pathogenic variants are exclusive to each MFS family, while only 10%–15% of variants recur between different families.<sup>5</sup> The *FBN1* protein undergoes cysteine substitution via a missense mutation, which is the most common pathogenic variant. Other types of mutations include nonsense mutations, deletions, insertions, various types of splice site mutations, and rarely large deletions of *FBN1*.<sup>6</sup> According to data from the Universal Mutation Database (UMD, <http://www.umd.be/FBN1>), more than 1500 pathogenic variants have been reported in the *FBN1*. The *FBN1* gene contains 66 exons, located at the 15q21.1 chromosomal region, and encodes the *FBN1* protein, a large extracellular matrix (ECM) glycoprotein (2871 aa, >350 kDa) that is highly conserved among different species. One of the most reliable and enduring associations between genotype and phenotype occurs when the mutation disrupts the cysteine residue, resulting in ectopia lentis. MFS patients with mutations that cause premature termination of translation are more prone to skeletal abnormalities, while ectopia lentis is less common.<sup>7</sup> Extracellular microfibrils, which are essential tissue components that endure repeated stretching and recoil, are primarily composed of *FBN1*. This protein is present in both elastic and nonelastic connective tissues throughout the body and is often closely associated with elastin fibers. *FBN1* plays an important role in the stability and strength of these tissues.<sup>8</sup> Microfibril production is disrupted by pathogenic *FBN1* variants, which also cause abnormal fibrillin protein formation and ultimately impair connective tissue.<sup>9</sup>

Here, we characterized the phenotype and determined the genetic etiology of a large Iranian family with symptoms consistent with MFS using molecular diagnostic methods. Through whole exome

sequencing (WES) and bioinformatics analysis, a heterozygous missense pathogenic variant (c.2179T>C) in *FBN1* gene was detected in the proband and affected family members. Moreover, we performed molecular docking to evaluate the effect of this variant on protein–protein interactions.

## 2 | MATERIALS AND METHODS

### 2.1 | Family presentation

Our proband (II:2, indicated by an arrow in the pedigree, Figure 1) was a 46-year-old female patient with general skeletal, visual, and cardiovascular problems who was referred to the genetic counseling center in Birjand in April 2023. The demographic information, detailed clinical data, and family history of the proband and her family were carefully assembled. She was the second sibling of non-consanguineous parents, originally from eastern Iran. The onset of ocular problems occurred when she was 20 years old with low visual acuity and slow progressive vision loss. The proband had a height of 178 cm and body mass index of 17 kg/m<sup>2</sup>. She had a history of heart and brain strokes and was regularly taking warfarin. The son of the proband (III:4), 16 years old, had a Marfan phenotype. He had various clinical features including mitral valve prolapse, orthodontic problems, thumb and wrist signs, pulmonary blebs (pneumothorax), striae distensae, and pectus deformity. The wrist signs of the proband and her son are shown in Figure 2A,B, respectively. The proband's echocardiography findings are shown in Figure 3C. The pedigree chart was created using Evagene pedigree drawing software (<https://www.evagene.com/>). Other family members (II:6, III:13, III:14, IV:1, IV:2, IV:3, and IV:4) had a normal phenotype. The procedure was approved by the Medical Ethics Review Board of Birjand Medical University (no. IR.BUMS.REC.1394.468) and the investigation was conducted in compliance with the principles outlined in the Declaration of Helsinki. Clinical and genetic evaluations were approved by the proband and family members, and informed consent was obtained from each participant.

### 2.2 | Clinical evaluations

The revised Ghent criteria were used for the proband and all suspected MFS-family members.<sup>10</sup> Certified clinicians conducted a detailed clinical history, laboratory tests, and standard physical examinations. The affected family members underwent cardiovascular evaluations, including cardiac ultrasonography and CT scans of the entire aorta. Chest and finger X-rays to evaluate the skeletal system. Moreover, routine ophthalmic examinations were performed by an experienced ophthalmologist, including visual acuity measurements, slit-lamp biomicroscopy, retinoscopy, tonometry, and fundus examination.

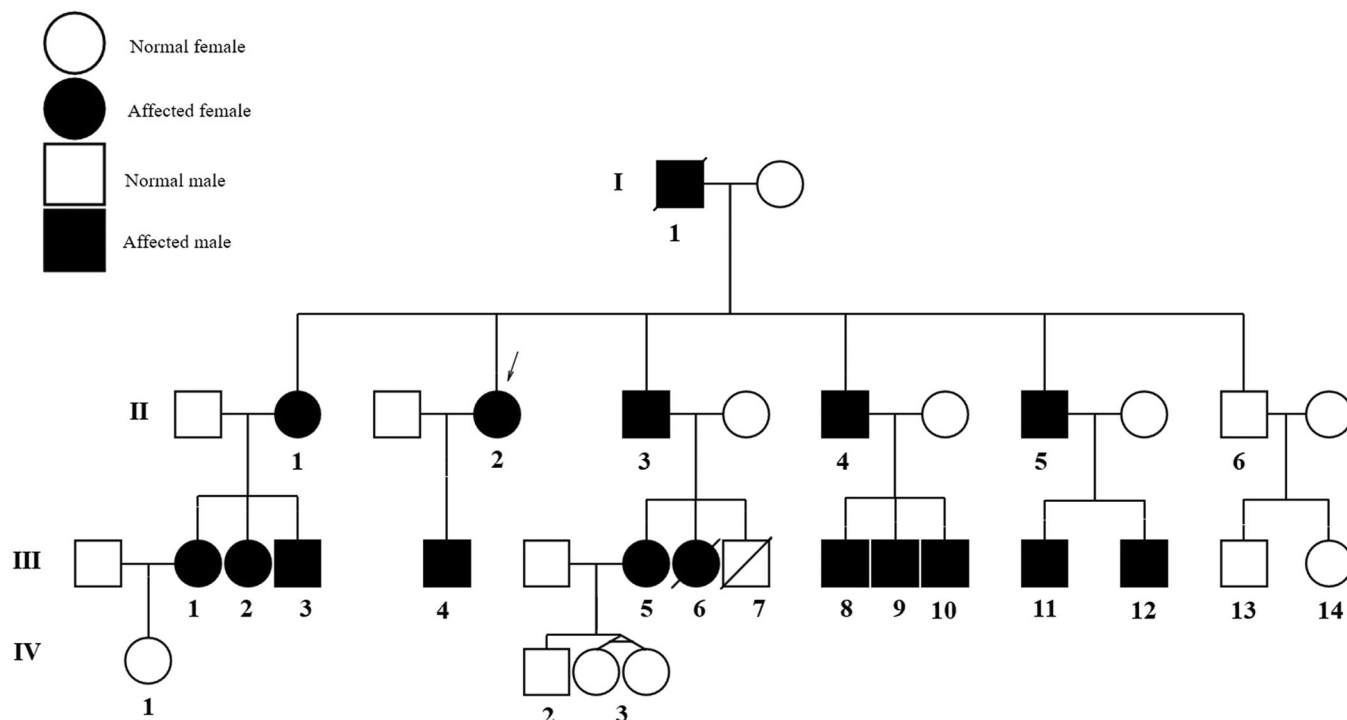


**FIGURE 1** Family pedigree of the proband. The proband is indicated with a small arrow. The diagonal line indicates deceased individuals. The black-filled symbols indicate family members with MFS. The unfilled symbols indicate normal family members. MFS, Marfan syndrome.

### 2.3 | Genetic evaluations

Peripheral blood samples from our affected proband, available family members ( $n = 14$ ), and 10 unrelated subjects with normal family history and phenotype were collected for DNA extraction. DNA was extracted from the lymphocytes using the phenol/chloroform method described by Miller et al.<sup>11</sup> The quality of the extracted genomic DNA was measured using an Epoch spectrophotometer (BioTek Inc.). To identify the genetic alterations causing this phenotype, we performed WES on the patient's (II:2) DNA sample. Exons were enriched, and the library was constructed using the Agilent SureSelect Human All Exon Version 6 Kit and TruSeq Exome Enrichment Kit. Libraries were sequenced using an Illumina NovaSeq 6000 instrument (Illumina) according to the manufacturer's standard operating protocols. The short reads obtained were aligned to the UCSC hg19 reference genome using the NovoAlign software package. Picard Toolkit v.2.14.0 (<http://picard.sourceforge.net>), and the FastQC software<sup>12</sup> (<https://bioinformatics.babraham.ac.uk>) were used to exclude duplicate reads and control the quality of reads, respectively. Sequence data conversion/indexing, variant determination, and functional annotation were performed using SAM (<http://samtools.sourceforge.net>), GATK v3.4.0 (Genomic Analysis Toolkit),<sup>13</sup> and ANNOVAR<sup>14</sup> toolkits. Rare variants with a minor allele frequency lower than 0.01 were screened using international online variant databases, including ExAC (<http://exac.broadinstitute.org/>), 1K Genome Project Phase 3 (<http://www.internationalgenome.org/data>), NHLBI ESP (Exome Sequencing Project, <https://evs.gs.washington.edu/EVS>), GME Variome (Greater Middle East, <https://igm.ucsd.edu/gme/>), and

Iranome (A catalogue of genomic variations in the Iranian, <http://iranome.ir/>) databases. The frequencies of the selected variants were checked in the Iranome database (<https://www.iranome.ir/>), and their clinical significance was determined using the ClinVar (<https://ncbi.nlm.nih.gov/clinvar/>), OMIM (Online Mendelian Inheritance in Man, <https://omim.org>), and HGMD (Human Gene Mutation Database, <http://hgmd.cf.ac.uk>) databases. To verify suspected pathogenic variants and perform cosegregation analysis, polymerase chain reaction (PCR) and bidirectional sequencing were performed on the patient and her available family members on an ABI 3730xl DNA analyzer (Applied Biosystems). We conducted Sanger sequencing to confirm mutation in the proband (II:2) and her son (III:4), and also, we analyzed the mutation in DNA samples from other available family members (13 individuals including II:1, II:3, II:4, II:5, III:1, III:2, III:3, III:5, III:8, III:9, III:10, III:11, and III:12) by ARMS-PCR. PCR amplification of the target DNA region was performed under the following standardized PCR conditions: initial denaturation at 95°C for 5 min (during the holding cycle), followed by 30 cycles of denaturation at 95°C for 15 s, annealing at 51°C for 30 s, and extension at 72°C for 30 s. A standardized master mixture (30  $\mu$ L) was prepared by combining 15  $\mu$ L of Taq DNA Polymerase 2X Master Mix Red (Ampliqon), 12  $\mu$ L of ddH<sub>2</sub>O, 1  $\mu$ L of DNA template, and 1  $\mu$ L of each forward and reverse primer (10 pM). Primer sequences were used for Sanger sequencing are summarized in Table 1. The sequencing results were analyzed using SnapGene Viewer v6.2.2 software (GSL BioTech LLC). Candidate variants and pathogenicity levels were determined according to ACMG/AMP standard guidelines.

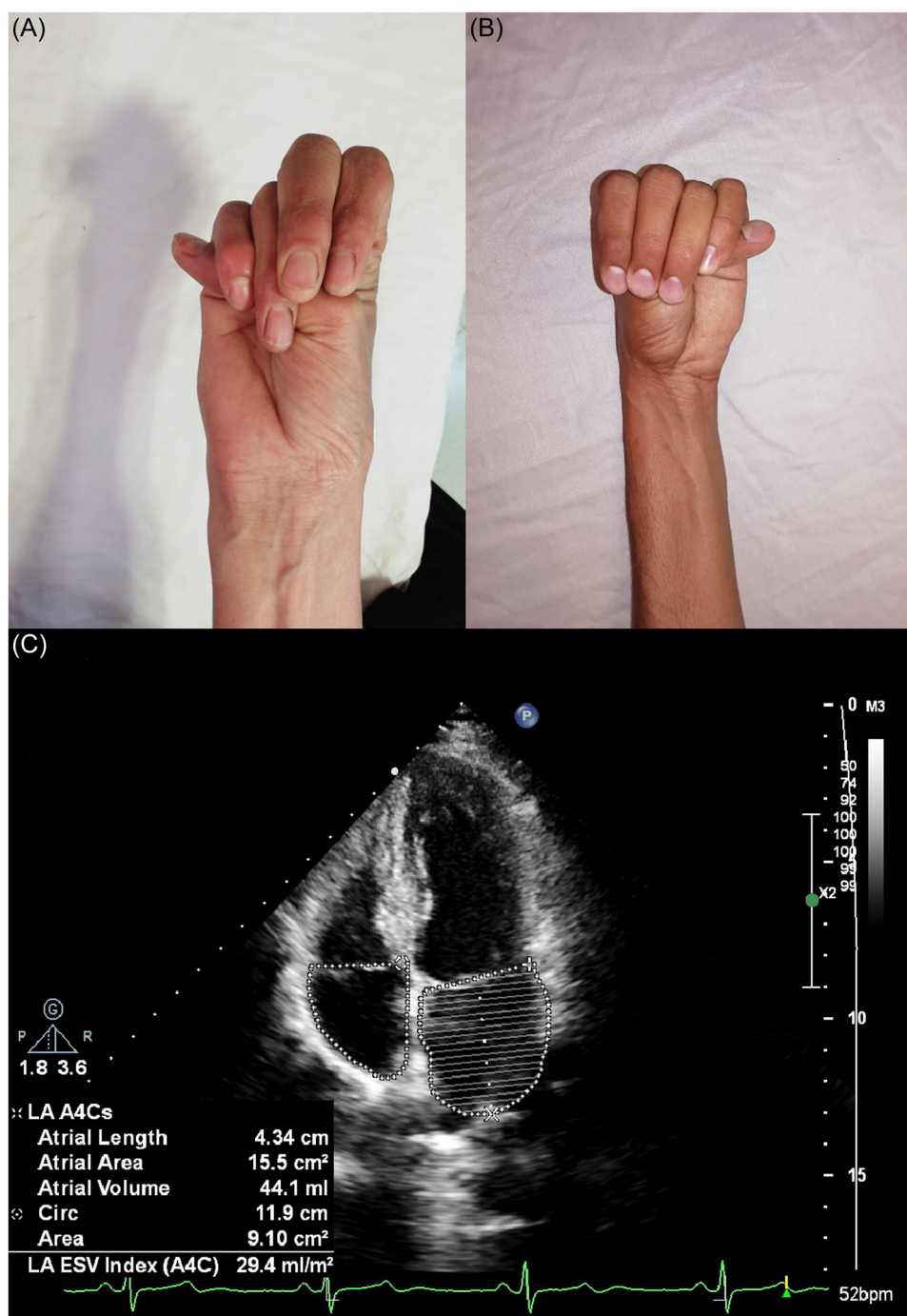


**FIGURE 2** Wrist sign in proband (A) and the affected son (B). Echocardiographic findings in the proband (C).

## 2.4 | Bioinformatic evaluations

To assess the possible effect of the identified variants on protein function, candidate variants were analyzed using several computational predictors, including PolyPhen-2 (Polymorphism Phenotyping version 2, <http://genetics.bwh.harvard.edu/pph2/>), MutPred (<http://mutpred.mutdb.org/>), FATHMM (<http://fathmm.biocompute.org.uk>), SIFT (Scale Invariant Feature Transform, <http://sift.jcvi.org/>), EIGEN, LRT (Likelihood Ratio Test), PROVEAN (Protein Variation Effect

Analyzer, [http://provean.jcvi.org/seq\\_submit.php](http://provean.jcvi.org/seq_submit.php)), and MutationTaster2 (<http://mutationtaster.org>). We used the Combined Annotation-Dependent Depletion (CADD) tool, available at <https://cadd.gs.washington.edu>, to evaluate the pathogenicity scores of the identified variants. Moreover, alignment of the FBN1 protein sequence among different species (human, mouse, Norway rat, cattle, chicken, rhesus, zebrafish, etc.) was performed using the EMBL-EBL Kalign tool<sup>15</sup> (<https://www.ebi.ac.uk/Tools/msa/kalign/>). Phylogenetic comparisons were performed to examine vertebrate

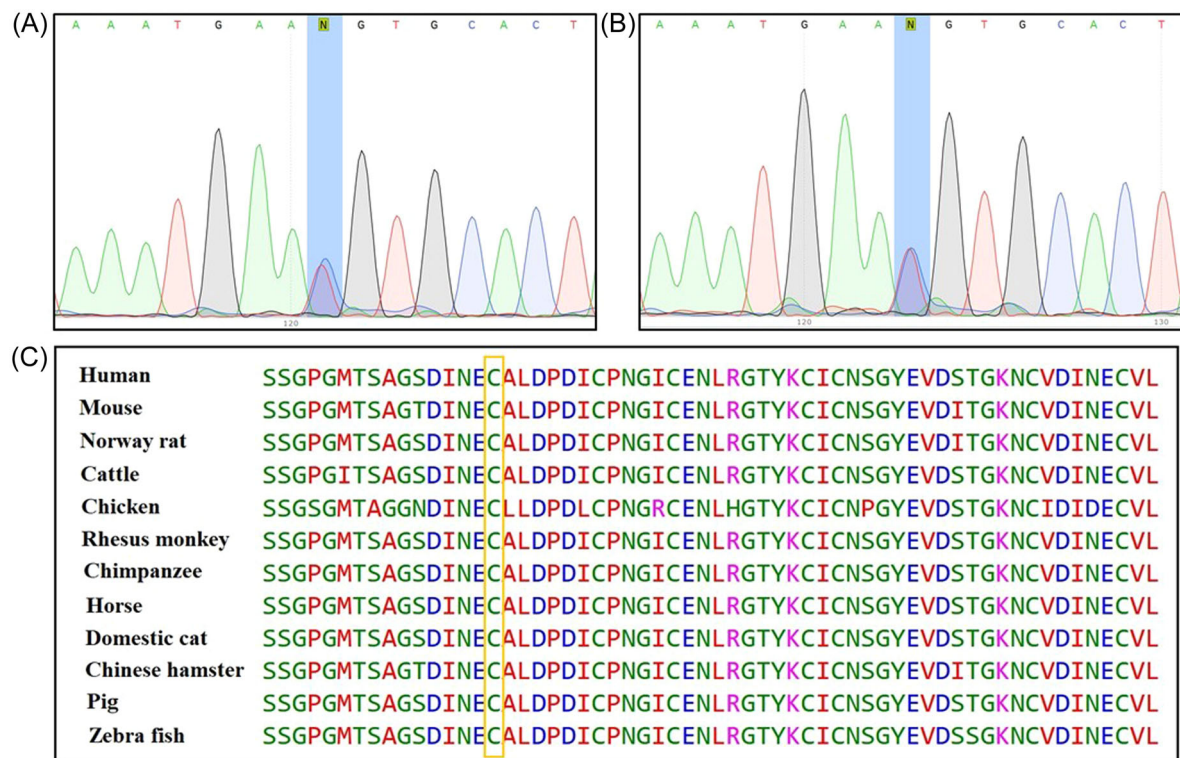


**FIGURE 3** Sanger sequencing results of proband (A) and affected son (B). Amino-acid alignment of *FBN1* protein sequences from different species using the following reference sequences: NP\_000129.3 (human), NP\_032019.2 (mouse), NP\_114013.2 (Norway rat), NP\_776478.1 (cattle), XP\_015147420.1 (chicken), XP\_014997668.1 (rhesus monkey), XP\_001149266.4 (chimpanzee), XP\_023473664.1 (horse), XP\_023111155.1 (cat), XP\_003506292.1 (Chinese hamster), XP\_003471907.1 (pig), and NP\_044923798.1 (zebrafish) (C). The results showed that position 727 of the protein sequence (C, cysteine) was located in a highly conserved region among different species.

**TABLE 1** The primers sequence characteristics and PCR condition for amplification of exon 19 of *FBN1*.

Gene	Primer sequence (5'→3')	Primer length (bp)	T <sub>m</sub> (°C)	Amplicon size (bp)
<i>FBN1</i> (exon 19)	Forward: GTATTATTTTATAATCTTAATTGATTTTGA	31	53	200
	Reverse: TTCAGAAAATGGGTAAACTTCT	23	54	

Abbreviation: PCR, polymerase chain reaction.

conservation using PhastCons100 (<http://compugen.bscb.cornell.edu/phast/>) and the PhyloP100 conservation tools. STRING Database v11.5 (<https://string-db.org/cgi/network>) was used to investigate for the physical protein–protein interactions of *FBN1* with other existing proteins.

## 2.5 | Molecular docking

Using the Iterative Threading Assembly Refinement (I-TASSER) server, we conducted *ab initio*/threading-based three-dimensional structure predictions for wild-type and mutant

*FBN1* proteins. The quality of the models was evaluated based on the confidence score (C-score), which ranged from  $-5$  to  $2$  and were considered acceptable. The RAMPAGE server was used to evaluate the secondary structure of the models. To determine the precise affinity between *FBN1* (wild-type and mutant) and latent transforming growth factor beta (TGF- $\beta$ ) binding protein 1 (LTBP1), we performed molecular docking and calculated the interaction energy using the HEX server. The PyMOL molecular graphics system was used to visualize possible interactions between the structural models. Sanger sequencing was performed to validate the newly identified potential causative variants.

### 3 | RESULTS

#### 3.1 | Clinical findings

A total of 17 related patients with a definite or suspected clinical diagnosis of MFS were recruited for the study. The patients included 11 males and six females, from one family in the South Khorasan Province (Figure 1). Physical, ophthalmic, and cardiovascular examinations were performed by an ophthalmologist and a cardiologist (Table 2). Patients present with a range of intricate symptoms, including cardiovascular, ocular, and skeletal abnormalities. All of these patients in the family manifested various visual problems, including iridodonesis (17/17), high intraocular pressure with ectopia lentis (17/17), cataracts (1/17), and blindness (3/17). Mitral valve prolapse and regurgitation followed by aortic root dilation were

observed in 16 of the 17 affected individuals. The general physical features of the patients included tall stature, arachnodactyly, disproportionately long and thin limbs, and joint laxity. The wrist signs in the proband and her son are shown in Figure 2A,B, respectively. The proband's echocardiogram results are shown in Figure 3C.

#### 3.2 | Genetic and bioinformatics findings

Using next-generation sequencing, we identified a novel missense variant (c.2179T>C, p.C727R, cDNA.2635T>C, g.148470T>C) in exon 19 of *FBN1* (GenBank NM\_000138.5). The transcript contains 66 exons and is annotated with 438 domains and features. This substitution indicates that TGT (Cys) changes to CGT (Arg) at codon

**TABLE 2** Clinical findings of the 17 affected members in the family.

Case ID	Age (year)	Gender	Cardiac disease	Skeletal abnormalities	Ocular abnormalities
I1	67 (deceased)	Male	+	+	+
II1	49	Female	+	+	+
II2	46	Female	+	+	+
II3	43	Male	+	+	+
II4	41	Male	+	+	+
II5	35	Male	+	+	+
II6	33	Male	-	-	-
III1	27	Female	+	+	+
III2	22	Female	+	+	+
III3	14	Male	+	+	+
III4	16	Male	+	+	+
III5	24	Female	+	+	+
III6	13 (deceased)	Female	-	+	+
III7	7 (deceased)	Male	-	-	-
III8	18	Male	+	+	+
III9	15	Male	+	+	+
III10	14	Male	+	+	+
III11	10	Male	+	+	+
III12	8	Male	+	+	+
III13	5	Male	-	-	-
III14	1	Female	-	-	-
IV1	4	Female	-	-	-
IV2	3	Male	-	-	-
IV3	1	Female (identical twins)	-	-	-

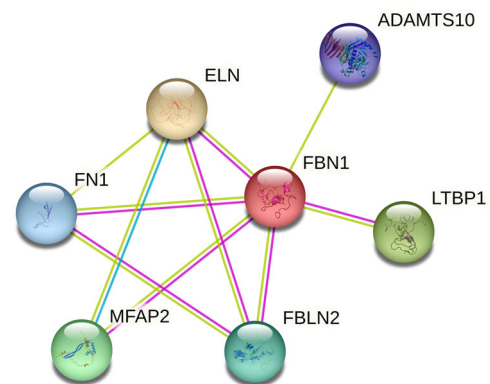
727 located on exon 19 in EGF-like 11, which is a calcium-binding domain and has been suggested as a disorder variant. The proband was heterozygous for this variant. The *FBN1* c.2179T>C variant has not been previously reported in the GME, ExAC, 1K Genome Project Phase 3, dbSNP, and Iranome databases. No previous description of the clinical significance of this variant has been found in clinical/genetic databases such as the Marfan database, ClinVar, HGMD, and OMIM. No other suspected or known variants with clinical significance were identified among the candidate variants. Subsequently, Sanger sequencing confirmed the mutation in the proband (II:2) and her affected son (III:4). Moreover, the presence of the mutation was determined by the ARMS-PCR method in other available family members (II:1, II:3, II:4, II:5, III:1, III:2, III:3, III:5, III:8, III:9, III:10, III:11, and III:12). They were also heterozygous, whereas no mutation was identified in his family members with normal phenotype. The sequencing results of the proband (exon 19 of *FBN1*) and her affected son are shown in Figure 3A,B, respectively. Based on the clinical data and genetic analysis, this missense variant was considered pathogenic. In silico analysis using several common web-based tools, such as PolyPhen-2, SIFT, PROVEAN, EIGEN, FATHMM, and Mutation Taster, predicted the p.C727R variant in *FBN1* with pathogenic effects and altered protein function or structure. Using the CADD tool (a web-based tool for scoring the deleteriousness of variants from 1 to 99), the c.2179T>C variant was predicted to be a pathogenic variant with a score of 34. A summary of the results obtained from the in silico investigation is presented in Table 3. Multiple alignments among different species revealed that cysteine amino acid 727 of *FBN1* is evolutionarily conserved in all investigated vertebrates (Figure 3C) and plays an important role in protein function. To detect the possible interactions between the *FBN1* protein and other existing proteins implicated in MFS pathogenesis, we searched the STRING database, as illustrated in Figure 4, and predicted a physical protein-protein interaction network. At an interaction score of 0.900, which represents the highest confidence level, the results revealed that the *FBN1* protein physically interacts with six other proteins. These proteins included *LTBP1*, *ADAMTS10*, *EL1*, *FN1*, *FBLN2*, and *MFAB2*. Understanding these interactions is essential to elucidate the molecular mechanisms underlying MFS and to help select candidate proteins for molecular docking studies with *FBN1*.

### 3.3 | Homology model building and molecular docking study

To better understand the molecular mechanics and structural consequences of the p.C727R mutation in *FBN1*, the online I-TASSER server was used to generate models of the EGF-like 11 domain, calcium-binding domain of Fibrillin, and C-terminal *LTBP1* fragment for the mutant and wild-type. Table 4 presents the accuracy estimation and Ramachandran plots of the wild-type and mutant models of the calcium-binding domain and the C-terminal *LTBP1* fragment. Ramachandran plots indicated that the majority of residues

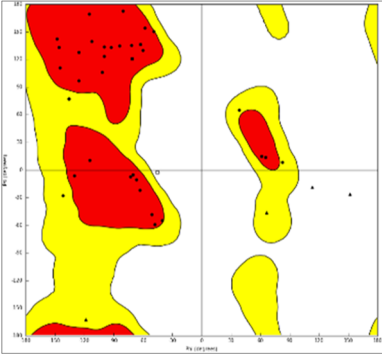
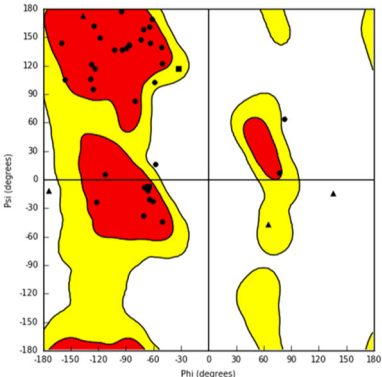
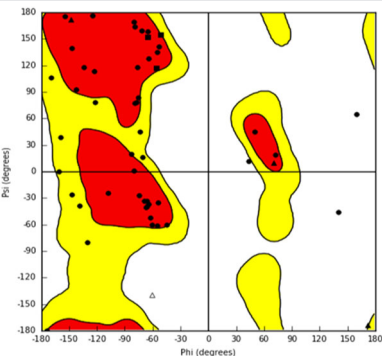
**TABLE 3** In silico prediction analyses of the *FBN1* c.2179T>C variant.

Algorithm	Prediction	Score
PhyloP100	Highly conserved	8.94
PhastCons100	Highly conserved	1.0
SIFT	Damaging	0.001
Polyphen-2	Probably damaging	0.997
LRT	Deleterious	0
PROVEAN	Damaging	-10.93
PrimateAI	Pathogenic	0.917
Mutation Taster	Disease causing	1.0
MutPred	Pathogenic	0.996
FATHMM	Damaging	-5.91
EIGEN	Pathogenic	1.082
M-CAP	Damaging	0.969
CADD	Deleterious	27
BayesDel addAF	Damaging	0.577
MetalR	Damaging	0.990
MetaSVM	Damaging	0.967



**FIGURE 4** Protein-protein interaction network between *FBN1* and other proteins using the STRING online database. At an interaction score of 0.900 (highest confidence score), the results showed that the *FBN1* protein interacted physically with six proteins, including *LTBP1*, *ADAMTS10*, *EL1*, *FN1*, *FBLN2*, and *MFAB2*. The purple lines: Strong and high-confidence interactions. Purple lines represent well-established and experimentally verified interactions. These interactions are highly reliable and are supported by robust experimental data. The light blue lines: Predicted interactions. The light blue lines in the STRING network represent interactions predicted based on computational methods, such as text mining, coexpression patterns, and database integration. These interactions are considered to have lower confidence than the experimentally verified. Green lines: Interactions based on neighborhood information. Green lines indicate interactions based on the physical proximity of proteins in the cell, which suggests that they may be functionally related. These interactions showed moderate confidence.

**TABLE 4** Estimated accuracy of FBN1 (wild and mutant) as well as LTBP1 models and Ramachandran plots.

Protein name	C-score	TM-score (mean $\pm$ SD)	RMSD ( $\text{\AA}$ )	Ramachandran analysis			
				Plots	Favored	Allowed	Outlier
FBN1-(wild)	0.37	0.76 $\pm$ 0.10	1.7 $\pm$ 1.5		33 (78.5%)	6 (14.4%)	3 (7.1%)
FBN1-(mutant)	0.30	0.75 $\pm$ 0.10	1.8 $\pm$ 1.5		35 (83.3%)	3 (7.2%)	4 (9.5%)
LTBP1	0.91	0.84 $\pm$ 0.08	1.2 $\pm$ 1.2		42 (76.4%)	9 (16.3%)	4 (7.3%)

Abbreviation: C-score, confidence score.

The C-score serves as a confidence metric for evaluating the quality of predicted models generated by I-TASSER. Its computation relies on the assessment of threading template alignments' significance and the convergence parameters derived from structure assembly simulations. The C-score is typically reported within the range of  $-5$  to  $2$ , whereby a higher C-score indicates a model with greater confidence, while a lower C-score suggests lower confidence in the model's accuracy.

TM-score is widely used for assessing structural similarity between protein structures, especially when the native structure is known. In our study, we utilized the C-score to estimate the TM-score of predicted models compared to native structures. This allowed us to determine the similarity or dissimilarity between the predicted models and native structures, providing insights into the accuracy of the modeling predictions. A TM-score  $>0.5$  indicates a model of correct topology and a TM-score  $<0.17$  means a random similarity. These cutoff does not depend on the protein length.

were in the favored region, with only a small number of outliers. To investigate the impact of the mutation on FBN1 binding, we conducted molecular docking studies using the Hex program (version 8.0.0). Figure 5 illustrates the docking results of FBN1 (wild-type and mutant) and LTBP1. Docking analysis revealed that substituting cysteine with arginine in the fibrillin led to a reduction of 23 kcal/mol. Furthermore, the results indicated that the binding pattern of the mutated Fibrillin was significantly distinct from that of the wild-type.

## 4 | DISCUSSION

MFS is a genetic disorder with high morbidity that affects connective tissue. It is caused by pathogenic variants of *FBN1* which can lead to serious life-threatening complications.<sup>16</sup> Due to the significant variability of MFS phenotypic expression within and between families, delayed clinical manifestation in older ages, the high rate of spontaneous mutations, and presentation similar to other



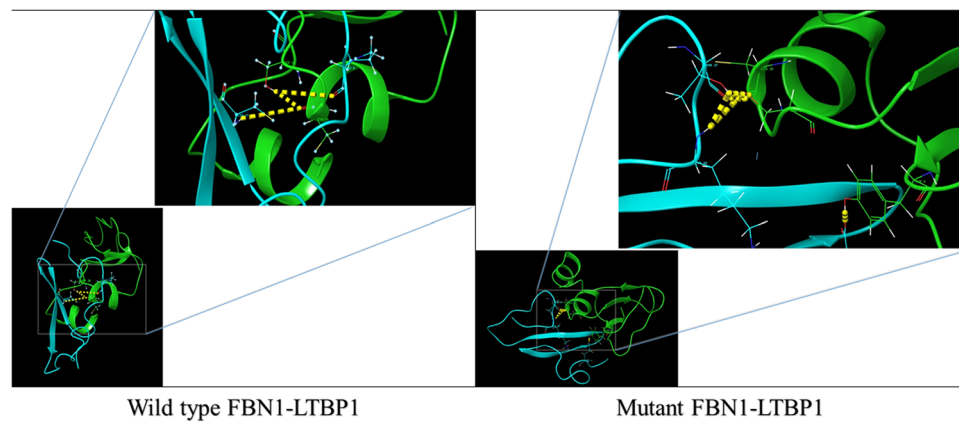


**FIGURE 5** Molecular docking of wild-type and mutant EGF-like 11; calcium-binding domain of FBN1 with C-terminal of LTBP1. The p.C727R residue in mutant EGF-like 11, the calcium-binding domain of FBN1 forms a polar (hydrogen) bond with p.K39 of LTBP1.

connective tissue diseases, diagnosing the condition can often prove challenging.<sup>17</sup> In this study, we evaluated the clinical features and genetic causes of MFS in a large Iranian family. Moreover, we used molecular docking to investigate the interaction between the mutated FBN1 protein and LTBP1 protein to understand how mutations can affect the binding interface and potentially disrupt the interaction between the two proteins.

The proband was a 48-year-old woman with physical, cardiac, and ocular abnormalities. The patient was phenotypically similar to other patients with MFS. She was the second daughter of a nonconsanguineous parent. Her older sister also had the same clinical symptoms, but was more severe. We found that family members exhibited a wide variety of clinical features, including skeletal, cardiovascular, and ocular abnormalities. The clinical variability of MFS is remarkable, even among members of the same family, with the first symptoms appearing as well as the extent and severity of clinical presentations.<sup>18</sup> Our findings were consistent with those of previous studies on MFS and emphasized the multisystemic nature of the disorder.

By evaluating all MFS patients in this large family, we found that mitral valve prolapse, regurgitation, and aortic root dilatation were the most common cardiovascular problems. Enlargement of the aortic root and proximal ascending aorta are the predominant cardiovascular problems observed in 80% of patients with MFS. This dilation can lead to aortic dissection, which is the primary cause of untimely mortality in these patients.<sup>19,20</sup>

Among the most prominent clinical findings in this cohort, the patients had cardiovascular issues with mitral valve prolapse and regurgitation. Additionally, aortic root dilation was present in the majority of affected individuals. The prevalence of aortic root enlargement, which can ultimately lead to aortic dissection, is consistent with previous reports, and highlights the importance of cardiovascular monitoring and intervention in patients with MFS. Early detection and management of aortic root dilation are pivotal for reducing the risk of life-threatening complications associated with MFS.

On the other hand, a remarkable finding in the ocular system of the family was ectopia lentis (17/17) and iridodonesis (17/17). Ectopia lentis is a hallmark ocular feature of MFS, which refers to the displacement or dislocation of the eye's natural lens from its normal position in the eye. Many studies have reported that myopia and ectopia lentis are the most prevalent ocular signs of MFS, observed in over 60% of the cases.<sup>21,22</sup> Other notable observations include early and severe myopia, retinal detachment, cataracts, glaucoma, flat cornea, and iris hypoplasia.<sup>22</sup> The high prevalence of ocular manifestations in our patients was consistent with well-established patterns of MFS, underscoring the necessity for regular ophthalmic evaluations in individuals with suspected or confirmed MFS.

We identified a missense pathogenic variant (c.2179T>C/p.C727R) in the *FBN1* gene of the proband and 16 other family members by genetic analysis. All the patients were heterozygous for the *FBN1* c.2179T>C variant. Genetic diagnosis serves as a crucial addendum to the proband's differential diagnosis, enabling a distinction between MFS and other syndromes, such as Shprintzen–Goldberg syndrome, Loey–Dietz syndrome, and vascular Ehlers–Danlos syndrome. Although they have similar clinical features, these conditions arise from mutations in various genes. This study also highlights the value of WES in genetic diagnosis and as a contribution to genetic counseling in families with MFS. WES has become a widely used laboratory test for diagnosing MFS, owing to its superior resolution and accuracy at the whole-genome level.<sup>23,24</sup> Identifying the genetic cause of MFS is crucial for accurate diagnosis, prognosis, and management of the disease. The use of WES has allowed for a more comprehensive evaluation of the genetic cause of the condition, which is especially important in cases where clinical diagnosis is not straightforward.

FBN1 is a large ECM protein that plays an important role in the formation and maintenance of elastic fibers. Elastic fibers are a primary component of connective tissues such as the skin, blood vessels, and lungs and provide elasticity and resilience to these tissues.<sup>25</sup> FBN1 interacts with a variety of proteins (Figure 4) to regulate the assembly and organization of elastic and fibrillin fibers

within the ECM.<sup>26</sup> One of the most well-known direct protein interactions of FBN1 is the glycoprotein LTBP1.<sup>26</sup> LTBP1 is a chaperone protein that binds and sequesters latent TGF- $\beta$ , which regulates cell proliferation and differentiation.<sup>27</sup> The interaction between FBN1 and LTBP1 is complex and multifaceted. This interaction is important for the correct localization and assembly of LTBP1 in the ECM.<sup>28</sup> FBN1 interacts with LTBP1 to target TGF- $\beta$  in the ECM and facilitate its activation. Disruption of LTBP1 function can lead to various connective tissue disorders.<sup>29</sup> Using molecular docking analysis, we found that the c.2179T>C/p.C727R variant located in the cbEGF domain of fibrillin, disrupts the interaction between FBN1 and LTBP1. Fibrillin contains EGF-like and cbEGF domains, which are responsible for binding to LTBP1. On the other hand, LTBP1 possesses an N-terminal domain followed by tandem repeats known as the TB domain, which interacts with fibrillin. The c.2179T>C/p.C727R variant of *FBN1* is a missense mutation that alters a single nucleotide in the DNA sequence and leads to substitution of the amino acid cysteine with arginine at position 727 in the FBN1 protein. This mutation is located at the C-terminal of the FBN1 protein, which is important for its interaction with LTBP1. This variant may potentially affect the formation of disulfide bonds in the calcium-binding domain of the EGF-like 11 protein, leading to a significant functional alteration in the affected domain and its adjacent domains. This mutation reduces the binding affinity between FBN1 and LTBP1, resulting in impaired TGF- $\beta$  activation and signaling. This may contribute to the pathogenesis of MFS, as dysregulation of TGF- $\beta$  signaling is a key feature of this disorder. Overall, the use of molecular docking to investigate the interaction between FBN1 and LTBP1 can provide valuable insights into the molecular mechanisms underlying their complex relationship and can help to identify potential targets for therapeutic intervention in connective tissue disorders.<sup>18,25,26,30,31</sup>

## 5 | CONCLUSION

In summary, we described a non-consanguinity MFS family with 17 affected members suffering from a rare pathogenic variant (c.2179T>C/p.C727R) in exon 19 of *FBN1*. Affected patients have various clinical features, including cardiovascular, ocular, and skeletal abnormalities. Clinical and genetic findings were consistent with a diagnosis of MFS, and *in silico* analysis predicted the pathogenic effects of the variant, suggesting alterations in FBN1 protein structure and function. These findings expand our knowledge of the genetic basis of MFS and highlight the significance of molecular genetic testing in the diagnosis and management of MFS. Additional investigations, especially functional studies, are warranted to validate the pathogenicity of the c.2179T>C/p.C727R mutation and elucidation of its precise molecular mechanisms in MFS. These results may have implications for clinical practice, potentially aiding in the diagnosis and management of MFS in affected individuals and their families. Molecular docking studies have suggested at altered binding

patterns resulting from mutation. Further exploration of these structural changes could deepen our understanding of MFS at the molecular level. This research may pave the way for the development of targeted therapies or diagnostic tools for MFS, offering hope to affected individuals.

## AUTHOR CONTRIBUTIONS

**Farzane Vafaeie:** Data curation; software; writing—original draft. **Zahra Miri Karam:** Investigation; methodology; software; writing—original draft. **Abolfazl Yari:** Formal analysis; investigation; methodology; software. **Hossein Safarpour:** Formal analysis; investigation; validation. **Tooba Kazemi:** Data curation; formal analysis. **Shokoofeh Etesam:** Conceptualization; data curation; resources. **Mojtaba Mohammadpour:** Data curation; methodology; resources. **Ebrahim Miri-Moghaddam:** Project administration; supervision; writing—review and editing. All authors have read and approved the final version of the manuscript.

## ACKNOWLEDGMENTS

We would like to thank the family of the patient for their participation and consent for data publication in this study.

## CONFLICT OF INTEREST STATEMENT

The authors declare no conflict of interest.

## DATA AVAILABILITY STATEMENT

The data that support the findings of this study are available on request from the corresponding author. The data, especially some clinical data, and patient images, are not publicly available due to privacy or ethical restrictions. The corresponding author (Ebrahim Miri-Moghaddam) had full access to all of the data in this study and took complete responsibility for the integrity of the data and the accuracy of the data analysis.

## ETHICS STATEMENT

This study was conducted in a manner compliant with the tenets of the Declaration of Helsinki. The Ethics Committee of Birjand Medical University gave its permission to our investigation (Ethics code: IR.BUMS.REC.1394.468). Written informed consent was obtained from all individual participants included in the study. All family members signed informed consent regarding publishing the clinical data.

## TRANSPARENCY STATEMENT

The lead author Ebrahim Miri-Moghaddam affirms that this manuscript is an honest, accurate, and transparent account of the study being reported; that no important aspects of the study have been omitted; and that any discrepancies from the study as planned (and, if relevant, registered) have been explained.

## ORCID

Ebrahim Miri-Moghaddam  <http://orcid.org/0000-0001-9435-2450>

## REFERENCES

1. Grange T, Aubart M, Langeois M, et al. Quantifying the genetic basis of Marfan syndrome variability. *Genes*. 2020;11:574. <https://www.mdpi.com/2073-4425/11/5/574/htm>
2. McKusick VA. Mendelian inheritance in man and its online version, OMIM. *Am J Human Genetics*. 2007;80(4):588-604. <https://pubmed.ncbi.nlm.nih.gov/17357067/>
3. Wright M, Connolly HM, Otto CMYS. *Genetics, Clinical Features, and Diagnosis of Marfan Syndrome and Related Disorders*. Elsevier; 2020. <https://www.medilib.ir/uptodate/show/8150>
4. Radonic T, De Witte P, Groenink M, et al. Critical appraisal of the revised Ghent criteria for diagnosis of Marfan syndrome. *Clin Genet*. 2011;80(4):346-353. <https://pubmed.ncbi.nlm.nih.gov/21332468/>
5. Chandra A, Patel D, Aragon-Martin JA, et al. The revised ghent nosology; reclassifying isolated ectopia lentis. *Clin Genet*. 2015;87(3):284-287. <https://pubmed.ncbi.nlm.nih.gov/24635535/>
6. Sakai LY, Keene DR, Renard M, De Backer J. FBN1: the disease-causing gene for Marfan syndrome and other genetic disorders. *Gene*. 2016;591(1):279-291.
7. Chen ZX, Jia WN, Jiang YX. Genotype-phenotype correlations of Marfan syndrome and related fibrillinopathies: phenomenon and molecular relevance. *Front Genet [Internet]*. 2022;13:493083.
8. Halper J. Basic components of connective tissues and extracellular matrix: fibronectin, fibrinogen, laminin, elastin, fibrillins, fibulins, matrilins, tenascins and thrombospondins. *Adv Exp Med Biol [Internet]*. 2021;1348:105-126. [https://link.springer.com/chapter/10.1007/978-3-030-80614-9\\_4](https://link.springer.com/chapter/10.1007/978-3-030-80614-9_4)
9. Peeters S, De Kinderen P, Meester JAN, Verstraeten A, Loeys BL. The fibrillinopathies: new insights with focus on the paradigm of opposing phenotypes for both FBN1 and FBN2. *Hum Mutat*. 2022;43(7):815-831. <https://pubmed.ncbi.nlm.nih.gov/35419902/>
10. Loeys BL, Dietz HC, Braverman AC, et al. The revised Ghent nosology for the Marfan syndrome. *J Med Genet*. 2010;47(7):476-485. <https://pubmed.ncbi.nlm.nih.gov/20591885/>
11. Miller SA, Dykes DD, Polesky HF. A simple salting out procedure for extracting DNA from human nucleated cells. *Nucleic Acids Res*. 1988;16(3):1215. <https://pubmed.ncbi.nlm.nih.gov/3344216/>
12. Andrews S. Babraham bioinformatics. FastQC: a quality control tool for high throughput sequence data. 2010. Accessed May 21, 2023. [https://scholar.google.com/scholar?hl=en&as\\_sdt=0%2C5&q=Andrews+S+%282010%29+FASTQC%3A+A+quality+control+tool+for+high+throughput+sequence+data&btnG=](https://scholar.google.com/scholar?hl=en&as_sdt=0%2C5&q=Andrews+S+%282010%29+FASTQC%3A+A+quality+control+tool+for+high+throughput+sequence+data&btnG=)
13. McKenna A, Hanna M, Banks E, et al. The genome analysis toolkit: a MapReduce framework for analyzing next-generation DNA sequencing data. *Genome Res*. 2010;20(9):1297-1303. <https://pubmed.ncbi.nlm.nih.gov/20644199/>
14. Wang K, Li M, Hakonarson H. ANNOVAR: functional annotation of genetic variants from high-throughput sequencing data. *Nucleic Acids Res*. 2010;38(16):e164. <https://academic.oup.com/nar/article/38/16/e164/1749458>
15. Lassmann T. Kalign 3: multiple sequence alignment of large datasets. *Bioinformatics*. 2020;36(6):1928-1929. <https://academic.oup.com/bioinformatics/article/36/6/1928/5607735>.
16. Milewicz DM, Braverman AC, De Backer J, et al. Marfan syndrome. *Nat Rev Dis Prim*. 2021;7(1):1-24. <https://www.nature.com/articles/s41572-021-00298-7>
17. Faivre L, Collod-Beroud G, Adès L, et al. The new Ghent criteria for Marfan syndrome: what do they change? *Clin Genet*. 2012;81(5):433-442. <https://pubmed.ncbi.nlm.nih.gov/21564093/>
18. Robinson PN, Arteaga-Solis E, Baldock C, et al. The molecular genetics of Marfan syndrome and related disorders. *J Med Genet*. 2006;43(10):769-787. <https://jmg.bmj.com/content/43/10/769>
19. Njoku P, Mbadiwe N, Onwubere B, et al. Marfan syndrome with aortic root disease, severe heart failure and aortic dissection—two case reports. *Niger J Clin Pract*. 2022;25(2):205-210. [https://journals.lww.com/njcp/Fulltext/2022/25020/Marfan\\_Syndrome\\_with\\_Aortic\\_Root\\_Disease,\\_Severe.15.aspx](https://journals.lww.com/njcp/Fulltext/2022/25020/Marfan_Syndrome_with_Aortic_Root_Disease,_Severe.15.aspx)
20. Sarr SA, Djibrilla S, Aw F, et al. Marfan syndrome and cardiovascular complications: results of a family investigation. *BMC Cardiovasc Disord [Internet]*. 2017;17(1):1-6. <https://bmccardiovascdisord.biomedcentral.com/articles/10.1186/s12872-017-0629-8>
21. Chen T, Deng M, Zhang M, Chen J, Chen Z, Jiang Y. Visual outcomes of lens subluxation surgery with Cionni modified capsular tension rings in Marfan syndrome. *Sci Rep [Internet]*. 2021;11(1):2994.
22. Shah S, Shah M, Chandane P, Makhloga S, Thorat D, Sanghani M. Clinical profile and outcome of ocular manifestation in Marfan syndrome in India. *Indian J Ophthalmol*. 2022;70(2):626.
23. Yang R, Zhang W, Lu H, et al. Identification of a novel 15q21.1 microdeletion in a family with Marfan syndrome. *Genetics Res*. 2022;2022:1-7.
24. Lin MR, Chang CM, Ting J, et al. Application of whole exome sequencing and functional annotations to identify genetic variants associated with Marfan syndrome. *J Pers Med*. 2022;12(2):198. <https://www.mdpi.com/2075-4426/12/2/198/htm>
25. Thomson J, Singh M, Eckersley A, Cain SA, Sherratt MJ, Baldock C. Fibrillin microfibrils and elastic fibre proteins: functional interactions and extracellular regulation of growth factors. *Semin Cell Dev Biol*. 2019;89:109-117.
26. Lockhart-Cairns MP, Cain SA, Dajani R, et al. Latent TGF $\beta$  complexes are transglutaminase cross-linked to fibrillin to facilitate TGF $\beta$  activation. *Matrix Biol*. 2022;107:24-39.
27. Gualandris A, Annes JP, Arese M, Noguera I, Jurukovski V, Rifkin DB. The latent transforming growth factor- $\beta$ -binding protein-1 promotes in vitro differentiation of embryonic stem cells into endothelium. *Mol Biol Cell*. 2000;11(12):4295-4308. <https://www.molbiolcell.org/doi/10.1091/mbc.11.12.4295>
28. Saharinen J, Hyytiäinen M, Taipale J, Keski-Oja J. Latent transforming growth factor- $\beta$  binding proteins (LTBPs)—structural extracellular matrix proteins for targeting TGF- $\beta$  action. *Cytokine Growth Factor Rev*. 1999;10(2):99-117.
29. Xiong Y, Sun R, Li J, Wu Y, Zhang J. Latent TGF- $\beta$  binding protein-1 plays an important role in craniofacial development. *J Appl Oral Sci*. 2020;28:20200262.
30. Godwin ARF, Dajani R, Zhang X, et al. Fibrillin microfibril structure identifies long-range effects of inherited pathogenic mutations affecting a key regulatory latent TGF $\beta$ -binding site. *Nat Struct Mol Biol*. 2023;30(5):608-618. <https://www.nature.com/articles/s41594-023-00950-8>
31. Robertson IB, Dias HF, Osuch IH, et al. The N-terminal region of fibrillin-1 mediates a bipartite interaction with LTBP1. *Structure*. 2017;25(8):1208-1221.

**How to cite this article:** Vafaeie F, Miri Karam Z, Yari A, et al. Clinical and genetic screening in a large Iranian family with Marfan syndrome: a case study. *Health Sci Rep*. 2023;6:e1647. doi:10.1002/hsr2.1647